

Towards idealized thermal stratification in a novel phase change emulsion storage tank

Haobin Liang^{a,c,1}, Liu Liu^{b,1}, Ziwen Zhong^a, Yixiang Gan^{c,*}, Jian-Yong Wu^{b,*}, Jianlei Niu^{a,c,*}

^a Department of Building Environment and Energy Engineering, The Hong Kong Polytechnic University, Hung Hom, Kowloon, Hong Kong

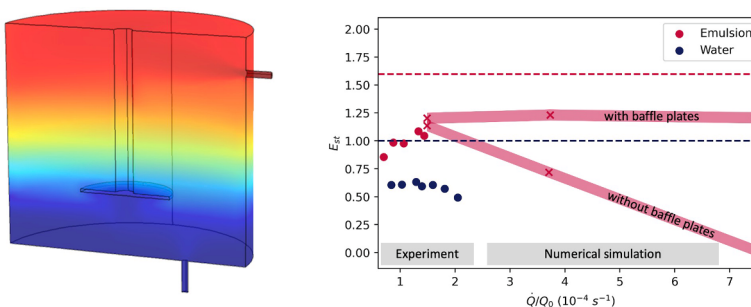
^b Department of Applied Biology & Chemical Technology, The Hong Kong Polytechnic University, Hung Hom, Kowloon, Hong Kong

^c School of Civil Engineering, The University of Sydney, NSW 2006, Sydney, Australia

HIGHLIGHTS

- We present a novel stratified phase change emulsion (PCE) tank for cold storage.
- Experiment results showed using 20 wt % PCE increases effective energy by 60–70%.
- A numerical model was developed for stratified PCE tank and validated.
- Numerical results show that baffles plates can significantly increase effective energy at high flow rates.

GRAPHICAL ABSTRACT



ARTICLE INFO

Keywords:
Stratification
Emulsion
Phase change material
Thermal energy storage

ABSTRACT

Energy storage density and charging/discharging speed are crucial performance indices for an energy storage unit. Phase change materials (PCMs) have been perceived to improve the energy storage density in thermal energy storage, but the relatively low charging/discharging speeds have been a bottleneck to their application. In building cooling storage applications using ice, the energy efficiency is compromised as the working temperature of ice storage is far below that required for air dehumidification and building cooling, which ranges between 7 and 17 °C. In this study, both experimental and numerical studies were carried out to demonstrate a novel stratified storage tank of PCM-in-water nano-emulsion for cold storage in building radiant cooling applications. A 20 wt% PCM-in-water nano-emulsion was utilized as both the storage medium and heat transfer fluid. The experimental results showed that the cooling capacity of a cooling panel was increased by 60% with phase change emulsion circulating in the loop. The effective energy storage capacity of the stratified storage tank was 1.6–1.7 times that of water in a wide range of discharging flow rates/speeds. Validated with the experimental data, the numerical simulation showed that installing baffle plates in the storage tank could effectively reduce the fluid mixing and significantly increase the effective energy storage capacity, especially at high discharging flow rates/speeds. In comparison with other PCM thermal energy storage designs, the stratified storage tank of PCM-in-water nano-emulsion has the advantage of a lower temperature difference between the cooling source and the demand, and thus raising the overall system energy efficiency.

* Corresponding authors.

E-mail addresses: yixiang.gan@sydney.edu.au (Y. Gan), jian-yong.wu@polyu.edu.hk (J.-Y. Wu), jian-lei.niu@polyu.edu.hk (J. Niu).

¹ These two authors contributed equally to the work.

Nomenclature		Subscripts
c_p	specific heat capacity,J/(kg•K)	dis displacement
D	tank diameter,m	e emulsion
E_{st}	effective energy ratio, -	eff effective
H	latent heat,J/kg	in inlet
k	thermal conductivity,W/(m•K)	w water
L	tank height,m	o outlet
Q	accumulative extracted energy,J	p plate
Q_{eff}	effective energy,J	t tube
Q_0	theoretical energy,J	
\dot{Q}	discharge power,W	
t	time,s	
t^*	dimensionless time, -	
T	temperature,K	
T_0	initial temperature,K	
u	fluid velocity,m/s	
V	tank volume,m ³	
\dot{V}	flow rate,m ³ /s	
		Greek letters
		ρ density,kg/m ³
		μ viscosity,Pa•s
		Abbreviations
		PCE phase change emulsion
		PCM phase change material
		SWS stratified water storage
		TES thermal energy storage

1. Introduction

Under rapid economic growth and social development, the application of renewable energy is increasing worldwide in recent years, to meet the growing energy demand and to realize environmental pollution abatement. However, the renewable energy supply such as solar and wind is unstable due to the intermittent nature of daily and seasonal weather conditions. Therefore, the integration of energy storage is crucial to alleviate the imbalance between energy demand and supply [1]. Thermal energy storage (TES) can compensate for the discrepancy of solar energy supply and demand by storing the energy received during the daytime to be used during nighttime. For instance, TES can ensure a stable supply of domestic solar hot water and manage the mismatch by extending the operation time of thermal power plants. TES can also be applied to peak shaving of power grids by storing energy in advance during off-peak periods of electrical load and releasing it during peak periods of electricity consumption. An example is that the TES system could make use of the low electricity cost during inactive nocturnal hours with chillers, which can be utilized for HVAC systems in the commercial buildings during on-peak hours in the daytime [2,3] or for cooling electronic devices in data centers [4].

Stratified storage tanks have emerged in recent years as a popular choice for TES and have been applied to solar energy utilization systems, such as solar water heating [5–7] and concentrated solar power [8]. Because of the low cost, non-toxicity, easy availability, high thermal capacity, and other advantages, water is widely used as the storage medium [5]. Thermal stratification is driven by thermal buoyancy force, due to the temperature difference between the hot and cold fluid. The thermal stratification in storage tanks could improve the efficiency of solar collectors and the quality of water delivered [7]. However, a fully stratified tank is not easy to obtain in practice, as the destruction of thermal stratification could occur due to the inlet mixing and local turbulence [5]. Therefore, the reduction of mixing between hot and cold fluid will enhance the thermal storage performance, leading to more effective thermal energy utilization.

Much effort has been made to minimize the mixing effect and to obtain maximum energy with baffles plates [8–12], equalizers [13], porous manifolds [7], diffusers [14,15] and perforated or slotted inlet [16,17]. With proper design the fluid would enter the tank with a lower velocity, leading to less mixing and thus promoting thermal stratification. For example, the baffle plates can effectively decrease the impingement and guide the direction of the coming fluid [5]. Altuntop

et al. [9] numerically investigated cylindrical, semi-cylindrical and conic obstacles and found that the designs with a gap in the center showed better thermal stratification. Bouhal et al. [10] recommended middle and top position and optimal angle for a flat plate. In general, all these approaches are effective to attain a more stable stratification, as indicated by higher MIX number, Richardson number, charging/discharging efficiency and exergy efficiency. Besides, thermal stratification depends on tank configurations and operating conditions. Ivers and Lin [18] numerically found that a larger aspect ratio of the tank allows hot water to build up at the top more quickly and thus reduces the mixing level. However, the surface area increases with increasing aspect ratio, resulting in more heat losses and making it impractical for installation. As for the flow rate, a higher value would generally induce strong jet flow from the inlet and destroy thermal stratification. With an inlet design like an equalizer, there may be an optimal flow rate maximizing the exergy efficiency [13].

Apart from integrating additional components or working on tank structure and operation conditions, submerging phase change materials (PCMs) into the thermal storage tank is another approach to improve thermal efficiency [6]. Compared with sensible energy storage, PCMs are receiving more attention these days for their much higher enthalpy change due to latent heat during phase transition. For conventional latent heat TES systems, PCM is confined in a stack of flat channels [19], placed in the shell side of a shell-and-tube unit [20] or macro-encapsulated as the packed bed [21], with heat transfer fluid passing through PCM.

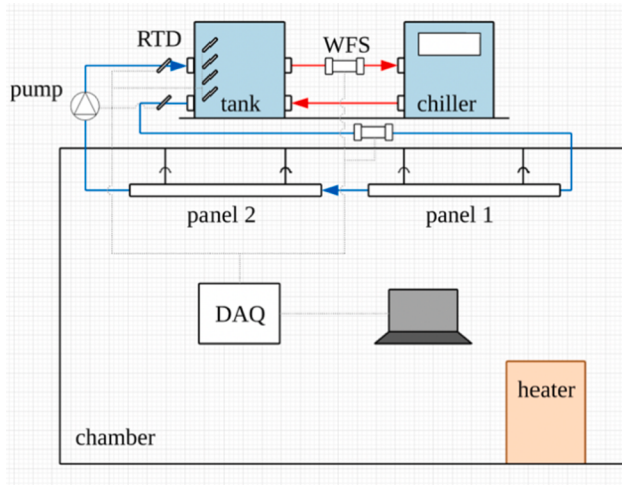
Different from traditional TES systems with PCM, phase change emulsions (PCEs) could be utilized as both storage media and heat transfer media. PCEs are fabricated by dispersing PCM as droplets in a carrier fluid, such as water, with the help of surfactants. Compared with the microencapsulated PCM slurries, PCEs have good operation stability and negligible thermal resistance of surfactant layer and are less likely to cause pipeline blockage [22]. Numerous studies have focused on improving the stability [23,24], reducing the supercooling [23,25,26], assessment of the rheological behaviors [27–29], and heat transfer characteristics in circular tubes [30,31], a rectangular mini-channel [32] and in a storage tank with water flowing in helical coils [33]. Using PCEs as a heat transfer fluid may reduce the equipment size such as heat exchanger, storage tank and piping units, and thus decrease the capital and operating costs. With a higher convective heat transfer coefficient, the latent functionally thermal fluids like PCEs have a great potential in HVAC systems [34], solar energy utilization [35] and

battery thermal management [36].

In cold storage applications, charging and discharging speeds are crucial to latent heat storage performance. However, the low thermal conductivity of PCM usually results in a low heat transfer rate, and thus a longer charging/discharging time [37]. Therefore, techniques have been employed to enhance the heat transfer of PCM, including fins, metal foams, nanoparticles [38–42]. For the charging process, several reported studies on different PCM heat exchangers concluded that a larger temperature difference and a larger flow rate are beneficial to shorten the charging time and thus increase the charging rate [43,44]. They specify the characteristic time when the stored energy reaches a certain percentage of the maximal storable energy, e.g. 90%. But for the discharging process, not all the stored energy can be extracted. The concept of cutoff temperature, depending on the specific application, is important to determine the useful energy that can be utilized. For example, the temperature of the fluid to cool the radiant cooling panels should not exceed a certain value to ensure the cooling capacity and thermal comfort. Therefore, in discharge, the effective energy capacity is also important besides the discharging rate. However, studies on the shell-and-tube PCM design showed that the increase in discharging rate under a higher mass flow rate negatively impacted the effective energy

storage capacity. The decreased effective storage capacity can be explained by the fact that at low effective thermal conductivities, the thermal resistance of PCM is much larger than that in heat transfer fluid [39,45]. Hence, there remains a gap in solving the trade-off between discharging energy capacity and discharging rate for TES systems utilizing PCM. Unlike in shell-and-tube units whose performance could be limited by the high thermal resistance on the PCM side, such an issue does not exist in PCM emulsion tank as the PCM is dispersed into the fluid. Therefore, the PCM emulsions have the potential of maintaining a stable effective storage capacity when the flow rate is changing.

In this work, a novel approach utilizing PCM emulsion in the stratification tank was proposed, which can reach a higher discharging rate with stable effective energy capacity at higher flow rates by introducing baffle plates. The PCM emulsion was used as the storage media for the thermal stratification tank, while circulating as the heat transfer media in a cooled ceiling system. The stratification of the PCM emulsion storage tank was tested through experiments and the effective energy efficiency Q/Q_0 , effective energy storage ratio E_{st} and discharging speed was investigated. Furthermore, a numerical model considering the phase change process in the PCM emulsion was developed, validated and applied for the stratification improvement with baffles near the



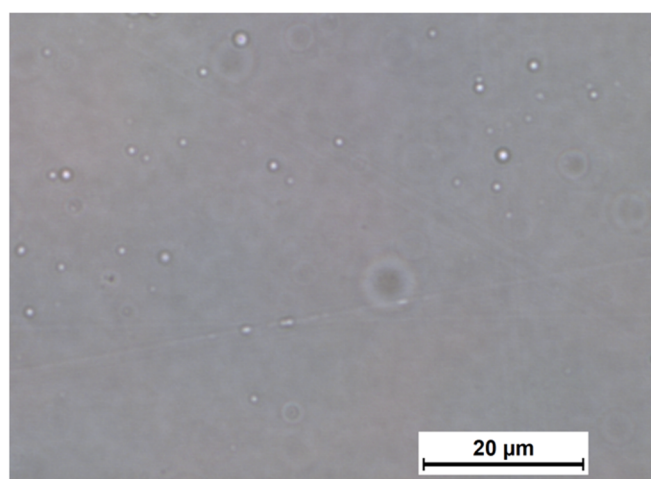
(a)



(b)



(c)



(d)

Fig. 1. Experimental set-up: (a) schematic diagram (RTD: resistance thermometer detector, WFS: water flowrate sensor, DAQ: data acquisition); (b) photograph of cold storage tank and chiller; (c) phase change emulsion; (d) micrograph of optical microscope.

inlet. To the best of our knowledge, this is the first study on a stratified phase change emulsion storage tank, demonstrating the PCM emulsion as a promising alternative for thermal energy storage.

2. Methodology

2.1. Experimental set-up

The experiment aims to investigate the thermal stratification of the phase change emulsion developed for the cooled ceiling application. Besides, the influence of the discharging flow rate on the stratification performance of the phase change emulsion storage tank and water storage tank has been researched.

Fig. 1 (a) shows the schematic diagram of the experimental setup, which mainly composes the thermal storage tank, chiller and two cooled ceiling panels. As shown in **Fig. 2**, the cylindrical stainless steel storage tank was 450 mm tall and the diameter was 590 mm. The fluid inside the tank (phase change emulsion or water) had a capacity of 44 L. A stirrer was designed for sampling and regeneration of the emulsion, which was turned off when the thermal storage tank is working during the discharging process, to avoid destroying the stratification inside the tank. The bottom of the storage tank was insulated with 15-mm thick high-density polyurethane foam, which had a thermal conductivity of 0.024 W/(m·K). The tank had an inlet and an outlet tube with an inner diameter of 15 mm and an outer diameter of 23 mm. The chiller was designed for phase change emulsion, with a cooling power of 0.93 kW and a working temperature range of 5–40 °C. Two SAS330 radiant cooling panels were placed in a chamber with dimensions of 2.9 m (height) × 2.7 m (width) × 4 m (length).

Copper tubes with a total length of 25 m were used to connect components of the experimental setup, which all had an inner diameter of 10 mm and were insulated with high-density polyurethane foam. The constant flow was guaranteed by the diaphragm metering pump and the flow rate was calibrated. To measure the temperature, PT-100 sensors were placed in the system, with an accuracy of ± 0.2 °C. The temperature of the inlet and outlet in the stratified tank were collected by Meacon datalogger, which recorded the fluid temperature every second. All the other temperature sensors were connected to the Honeywell IQ®4E data acquisition system and the data were recorded every minute. The positions of temperature sensors distributed along the axial direction inside the storage tank are shown in **Fig. 2**, which were used to capture the thermal stratification characteristic and to validate the numerical

model.

Fig. 1 (b) and (c) show the photograph of the experimental set-up, which includes the cold storage tank, chiller and phase change emulsion used in this study. The PCM used in the experiment is pure n-alkanes from Tokyo Chemical Industry Co., Ltd. (TCI) Japan. The phase change emulsion is composed of n-hexadecane (C16, 99%) as PCM agent and water as the base fluid. Besides, n-alkane n-octacosane (C28, 98%) was added as a nucleating agent to reduce supercooling and surfactant was added for stability. For the low-energy method including the phase inversion temperature (PIT) method used in this work to prepare the emulsion, paraffin is regarded as the most suitable candidate because it can be encapsulated more efficiently with nano-droplets and ensure the stability of the emulsion, compared with other options including nanoparticles and organic derivatives. When C16 is chosen as the PCM agent for phase change emulsion, pure n-alkanes with a higher melting temperature are the most ideal candidates as the nucleating agent. We tested three pure n-alkanes including n-tetracosane (C24), n-octacosane (C28) and n-dotriacontane (C32) and they showed similar performance in reducing the supercooling. In the end, n-octacosane (C28) is used as the nucleating agent in this work. The 20 wt% PCM nano-emulsion was used as the stratified storage medium in the tank. **Fig. 1** (d) shows an optical microscope image of 20 wt% PCE. The average droplet size in the emulsion is less than 100 nm, and the detailed size distribution can be observed by dynamic laser scatter (DLS). In addition, the phase change emulsion has relatively low viscosity and high stability. More details on the preparation and properties of the nano-emulsion can be found in previous literature [25].

2.2. Experiment procedure

At first, the chiller was turned on to cool down the stratified thermal storage tank. Cold fluid was pumped into the tank from the bottom and circulated back to the chiller from the top. After 1–1.5 h, the chiller reached the minimum temperature of 5 °C and inside the stratification storage tank, the fluid temperature distributed evenly along the vertical direction. This could be determined by the four temperature sensors placed in the tank when the maximum temperature difference was less than 0.2 °C. Then, the chiller was turned off and the pump in the discharging cycle was turned on. During the discharging process, hot fluid circulated back to the top of the tank and cold fluid at the bottom was pumped out to cool down the ceiling panels, so that the thermal stratification in the tank could be developed.

At the start of the discharging experiments, the emulsion or water in the tank temperature was cooled by the chiller to 5.5 ± 0.3 °C, to ensure the same initial temperature T_0 under different fluid flow rate conditions. The inlet temperature was maintained at 15.5 ± 0.5 °C by controlling the heat load released from heaters to ceiling panels in the chamber. The data were collected until the outlet temperature of the tank is larger than 13 °C.

The flow rates carried out during the discharging process were 0.194 L/min, 0.242 L/min, 0.296 L/min, 0.370 L/min and 0.401 L/min for emulsion, and 0.242 L/min, 0.296 L/min, 0.370 L/min, 0.401 L/min, 0.456 L/min, 0.518 L/min and 0.584 L/min for water. As the inlet temperature of was controlled as constant around 15.5 °C in experiments, to compare the storage performance, the flow rate cannot be either too high or too low. Otherwise, the inlet temperature would be lower or higher than the expected. Once the range of flow rates was determined, experiments of several flow rates inside this range were carried out. Each set of flow rate was conducted three times for the experiment repeatability. It is worthwhile to mention that the system with water could operate under higher flow rates than the one with phase change emulsion. This is because the inlet temperature of phase change emulsion returned from the ceiling panels was lower than the one of water under the same flow rate, due to the latent heat. To keep the inlet temperature a constant, more heat loads were required to be added into the chamber with phase change emulsion as the heat transfer fluid.

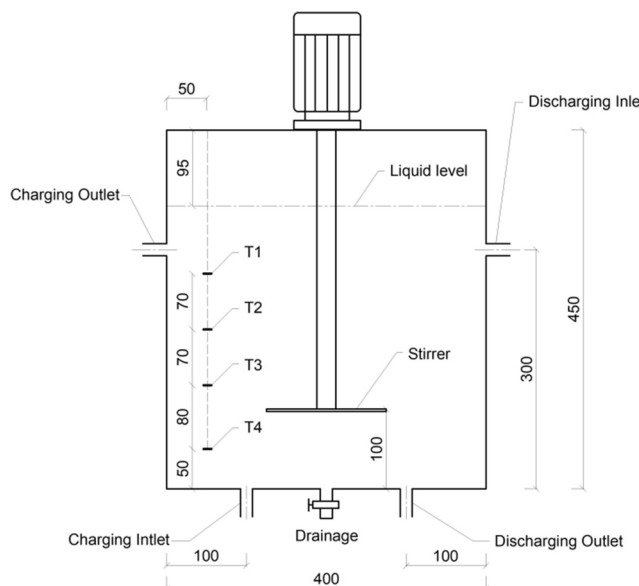


Fig. 2. Design parameters of storage tank.

However, it was unsafe for the system operation if the chamber temperature was too high. Therefore, the maximal flow rate of the emulsion was 0.401 L/min, lower than the one of water.

2.3. Numerical model

The numerical study aims to examine the model validity to simulate the phase change emulsion behavior in a stratification storage tank, and to exhibit the outcomes of increasing thermal performance of a phase change emulsion storage tank by enhancing the thermal stratification level. Fig. 3 (a) illustrates the 3D computational domain of the phase change emulsion storage tank, built in the commercial software COMSOL [46] and Fig. 3 (b) shows the temperature distribution in the 3D space. Since the temperature distribution at the symmetry plane of the thermal storage tank is representative of the stratification, our results analysis focus on the symmetry plane in the following section. Half of the cylindrical tank with the stirrer inside was modeled when the flow rate was 0.4 L/min for the discharging process. The hot emulsion enters the inlet port at the top and the cold emulsion exits from the outlet port at the bottom.

The geometric parameters of the tank are determined as specified in Section 2.1. The length of the inlet and outlet ports are both 50 mm. The existence of a stirrer is taken into account in the numerical model to better simulate the fluid behavior, the geometry of which is subtracted from the tank geometry through Boolean operation. The operation can subtract one block from the other one and form a single new block, and thus the fluid flow excluding the stirrer can be simulated in the model. The stirrer consists of a cylinder with a diameter of 30 mm and a length of 100 mm, and another one with a diameter of 150 mm and a length of 5 mm.

Fig. 4 shows the DSC results of phase change emulsion with and without the nucleating agent during the cooling and heating process. It could be observed that the addition of nucleating agent significantly reduces the supercooling. For the emulsion used in the experiment (2.5 wt%), the onset temperature is 10.0 °C and 12.8 °C for cooling and heating respectively, while the peak temperature is 9.0 °C when cooling and 14.1 °C when heating. The latent heat is 38.0 kJ/kg when PCM solidifies and 32.0 kJ/kg when PCM melts. The properties of phase change emulsion are shown in Table 1. Given the dynamic viscosity at 5 °C and 25 °C obtained from a rotational viscometer (DV3T, Brookfield), the viscosity of the emulsion is assumed as a linear function in the temperature range in the model. Thermal properties including latent heat and specific heat capacity were obtained from the DSC results, and the melting temperature was obtained from the combined DSC curve and heating curve. The thermal conductivity and density of phase

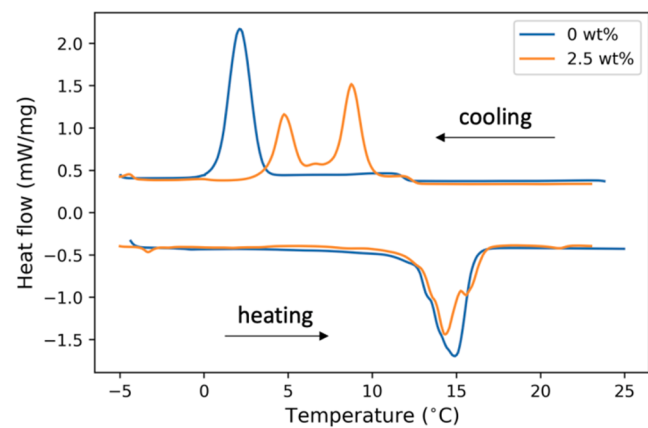


Fig. 4. DSC results of phase change emulsion with (2.5 wt%) and without (0 wt%) the nucleating agent.

Table 1
Properties of phase change emulsion (at 20 wt% PCM).

Property	Value
Melting temperature (°C)	12.5–14.5
Melting latent heat (kJ/kg)	32
Dynamic viscosity (mPa·s)	7.5 at 25 °C, 17 at 1 °C
Thermal conductivity (W/(m·K))	0.5
Specific heat capacity (J/(kg·K))	3700
Density (kg/m ³)	970 at 25 °C

change emulsion are calculated based on the mass fraction of PCM (n-hexadecane) and water. In the numerical model, the thermal conductivity and specific heat capacity are assumed as a constant, while the density is a function of temperature, to account for the thermal buoyancy effect in the tank. The phase change process is taken into account by assigning an effective specific heat capacity $c_{p,\text{eff}} = H/\Delta T$, which is the latent heat over the melting temperature ranges.

According to the flow rate of 0.4 L/min and tube diameter of 15 mm, the Reynolds number can be calculated as 45. Therefore, in COMSOL, Laminar Flow and Heat transfer modules were applied to simulate the transient hydrodynamic and heat transfer behavior of the phase change emulsion. The governing equations of mass, momentum and energy conservation are solved by the finite element method, summarized in Eqs. (1)–(3).

$$\rho(\nabla \cdot \mathbf{u}) = 0 \quad (1)$$

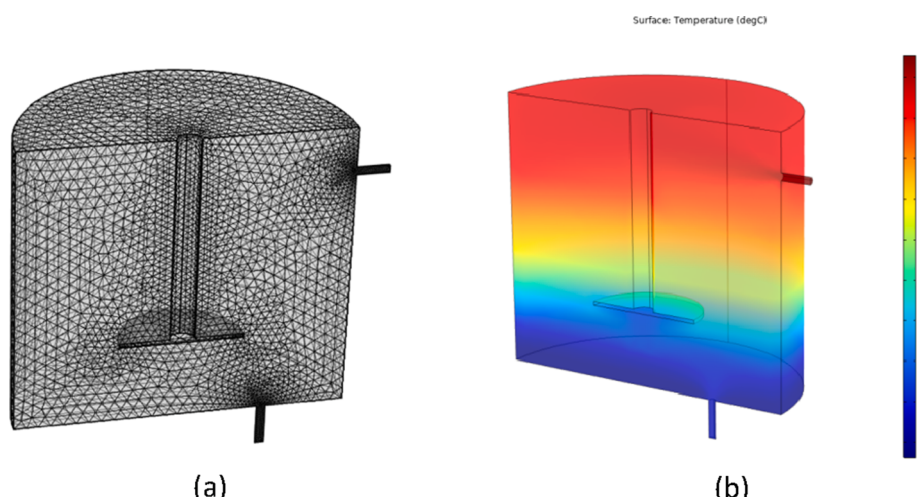


Fig. 3. The 3D numerical model of PCE storage tank: (a) unstructured grid; (b) temperature distribution.

$$\rho \frac{\partial \mathbf{u}}{\partial t} + \rho (\mathbf{u} \cdot \nabla) \mathbf{u} = -\nabla p + \mu \nabla (\nabla \mathbf{u} + (\nabla \mathbf{u})^T) + \rho g \quad (2)$$

$$\rho c_p \frac{\partial T}{\partial t} + \rho c_p \mathbf{u} \cdot \nabla T = \nabla \cdot (k \nabla T) \quad (3)$$

The uniform velocity and pressure were assigned as the inlet and outlet boundary conditions, respectively. The inlet temperature of 15.5 °C was specified as the thermal boundary condition. No-slip and adiabatic boundary conditions were applied on the wall surfaces of the tank and stirrer. Initially, no flow was within the tank and the emulsion was at the uniform temperature of 5.5 °C, the same as the experiment.

More grid elements were added where flow experienced significant changes, including inlet and outlet ports, and near the wall of the stirrer, as shown in Fig. 3. The mesh independence and time step independence were checked and computations were run with a time step of 0.5 s and grid element number of 172,123. The convergence criterion was set as when the residuals for equations fall under 0.0001.

The experimental data of T1-T4 temperature, when the emulsion flow rate is 0.4 L/min, were used to validate the numerical model. The 2-hour discharging process of the phase change emulsion tank was used to compare the predicted numerical results with experimental data. The 3D model is for analysis of the thermal stratification in the phase change emulsion tank during discharging. Besides the 3D model, a simplified 2D axisymmetric model was also developed to speed up the simulation process. This can help to illustrate stratification enhancement with baffle plates and to capture the storage behavior under higher flow rates (in Section 3.3). Fig. 5 shows the temperature variation with time of both models. The normalized root-mean-square deviations (NRMSE) between the experimental and numerical data are calculated by $\sqrt{\frac{\sum_{i=1}^n (T_{exp} - T_{num})^2}{n(T_{in} - T_{out})}}$, where T_{exp} is the temperature measured in experiments, T_{num} is the corresponding temperature at the same time from numerical simulation, n is the number of data points, T_{in} is inlet temperature and T_{out} is outlet temperature. NRMSE for 3D model from T1 to T4 shown in Fig. 5 (a) are 0.092, 0.061, 0.077 and 0.059, while the one for 2D model from T1 to T4 shown in Fig. 5 (b) are 0.047, 0.047, 0.058, 0.076. It could be observed that good agreement is obtained between experimental and numerical results. The difference could be due to the fact that the inlet temperature of the emulsion was fluctuating in a certain range in the experiment. Especially when it was approaching the end of discharging process, the temperature difference between inlet and outlet temperature was decreasing, making it harder to maintain the inlet temperature by controlling the heat load in the chamber. Thus, the inlet emulsion returned usually had a higher temperature than the expected average value. This is because in the discharging loop,

increasing outlet temperature greatly raised the emulsion temperature at the inlet port after gaining heat from the ceiling panels in the chamber. In comparison, the inlet temperature is kept constant in numerical simulation. On the other hand, in simulation the tank was assumed as perfectly thermally insulated, while in the experiment there could exist heat loss to the environment during the operation. This could also affect the temperature evolution discrepancy of the emulsion in the tank between numerical and experimental data.

The numerical model exhibits the validity of the effective heat capacity method to consider the phase change effect of PCM in the emulsion. Then it is applied to illustrate the concept of improving thermal stratification with tank design and used for further analyses of the energy storage performance of the phase change emulsion storage tank.

2.4. Dynamics of stratification during discharging

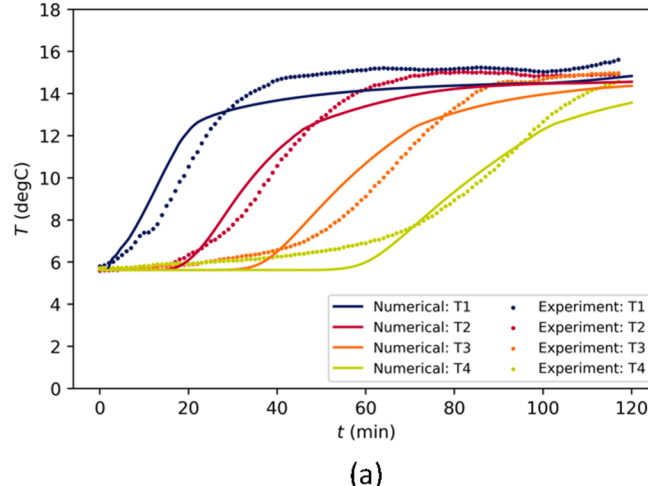
Thermal stratification can be assessed by miscellaneous methods, including Richardson number, stratification number, MIX number and exergy efficiency. However, some indices can be applied only under certain circumstances. For example, the MIX number is only useful for design comparisons with the same mass flow rate and thermal conditions [18]. As for the exergy analysis [13,18], the calculation requires the instantaneous value of enthalpy integrated over the tank volume. This is not available when phase change emulsion serves as the heat storage medium, as the effective specific heat capacity is not a constant all over the tank with varying temperature, due to latent heat. In this work, we introduced energy analysis based on the cutoff condition on outlet fluid temperature, to capture the dynamics and to measure the thermal stratification performance during the discharging process.

In this study, the time when the initial cold fluid is completely replaced by inlet hot fluid, is defined as the displacement time t_{dis} , which is the tank volume over the fluid flow rate, shown in Eq. (4). Hence, the duration of the discharging process could be measured by the dimensionless time t^* , which is introduced in Eq. (5). The dimensionless time describes the displacement progress by hot fluid while discharging, which is the ratio of the transient time over the displacement time.

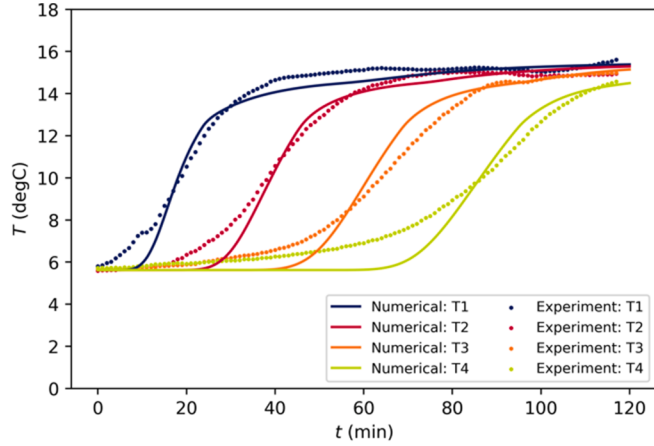
$$t_{dis} = \frac{V}{\dot{V}} \quad (4)$$

$$t^* = \frac{t}{t_{dis}} \quad (5)$$

Fig. 6 (a) characterizes the phase change emulsion stratification degree of a fully mixed, experimental, and perfectly stratified tank with



(a)



(b)

Fig. 5. Numerical model validation (flow rate: 0.4 L/min): (a) 3D model; (b) 2D axisymmetric model.

a plot of fluid outlet temperature over dimensionless time when the flow rate is 0.4 L/min. For a perfectly stratified tank, the temperature remains as the initial temperature until the displacement time t_{dis} and jumps to the inlet fluid temperature. As for the well-mixed scenario, the outlet temperature would be the same as the rest of the fluid in the tank, which could be estimated by the energy balance between the stored energy and inlet energy [47] and would increase with time relevant to the natural component term, shown in Eqs. (6) and (7). The stratification performance of the phase change emulsion in the experiment is between the ideal perfectly stratified case and the worst fully mixed case.

$$\rho V c_p \frac{dT}{dt} = (\rho \dot{V}) c_p (T_{\text{in}} - T) \quad (6)$$

$$T = T_{\text{in}} + (T_0 - T_{\text{in}}) e^{-\frac{t}{t_{\text{dis}}}} \quad (7)$$

It is important to identify the cutoff temperature for the outlet fluid as it defines the useful energy that could be extracted during the discharging process [19]. For example, there exists a maximum allowable temperature to maintain the cooling power and thermal comfort for the room cooling and to ensure the operation of computing devices for a data center cooling application. In this work, we determined the cutoff temperature with the heat transfer effectiveness $\eta = (T_{\text{in}} - T_{\text{out}})/(T_{\text{in}} - T_0)$ [20,48]. By assuming the minimum allowable η of 80 %, the cutoff temperature would be 7.5 °C, giving the effective dimensionless time t^*_{eff} . Given the inlet and outlet temperature, the stratification performance of the storage tank could be estimated through energy analysis. The theoretical energy of emulsion $Q_{0,e}$ stored at the beginning of

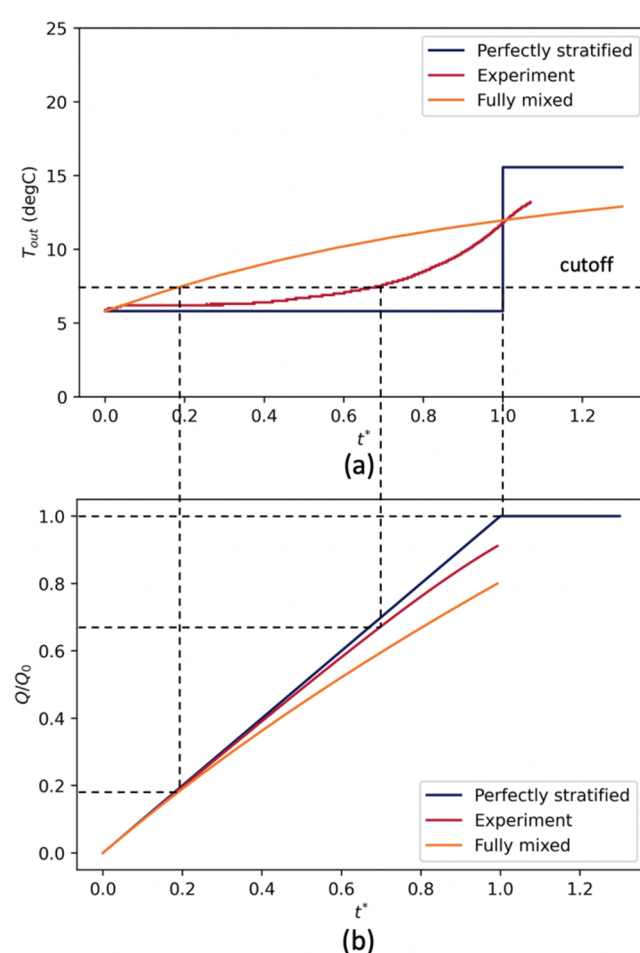


Fig. 6. Phase change emulsion stratification degree in fully mixed, experimental, and perfectly stratified tank (flow rate of 0.4 L/min): (a) outlet temperature T_{out} ; (b) energy efficiency Q/Q_0 .

discharge is the sum of the sensible heat and latent heat between initial temperature and inlet temperature, shown Eq. (8). The accumulative extracted energy Q used for the cooling of ceiling panels could be estimated by Eq. (9), in which the instantaneous energy q depends on inlet and outlet temperature, given in Eq. (10). The effective specific heat capacity $c_{p,\text{eff}}$ during the phase change process can be estimated by the latent heat over the phase change temperature range, i.e. $c_{p,\text{eff}} = H/(T_{\text{end}} - T_{\text{start}})$. Hence, the energy efficiency Q/Q_0 indicates the percentage of the stored energy that has been extracted for cooling during the discharging process. Fig. 6 (b) shows the variation of the energy efficiency over the dimensionless time. When the cold fluid in the tank is fully replaced by the inlet hot fluid, i.e. $t^* = 1$, 91% and 80% of the stored energy are released for the experiment and fully mixed scenario, respectively, close to the total stored energy Q_0 . However, the effective energy Q_{eff} is determined by the cutoff temperature, calculated based on the effective time t_{eff} . The figure shows that when the outlet temperature reaches the cutoff value, the effective energy Q_{eff} that is discharged and can be used for cooling is only 66% for the experimental stratified emulsion tank and 18% for fully mixed. This exhibits that how the stratification affects the energy performance of the storage tank and it is of great importance to enhance the stratification by avoiding fluid mixing in the tank during discharging process.

$$Q_{0,e} = \rho_e V (c_{p,e}(T_{\text{in}} - T_0) + H) \quad (8)$$

$$Q = \int_0^{t^*} q dt \quad (9)$$

$$q = \begin{cases} (\rho_e \dot{V}) (c_{p,e}(T_{\text{in}} - T_{\text{out}}) + c_{p,\text{eff}}(T_{\text{end}} - T_{\text{start}})), & T_{\text{out}} < T_{\text{start}} \\ (\rho_e \dot{V}) (c_{p,e}(T_{\text{in}} - T_{\text{out}}) + c_{p,\text{eff}}(T_{\text{end}} - T_{\text{out}})), & T_{\text{start}} < T_{\text{out}} < T_{\text{end}} \\ (\rho_e \dot{V}) (c_{p,e}(T_{\text{in}} - T_{\text{out}})), & T_{\text{out}} > T_{\text{end}} \end{cases} \quad (10)$$

Apart from the effective energy efficiency Q_{eff}/Q_0 , the effective energy ratio E_{st} [20,48] is also applied for energy analysis in this work. As shown in Eqs. (11)–(12), E_{st} indicates the performance of a thermal storage tank, when compared with an ideal stratified water storage (SWS) tank. The effective energy Q_{eff} is determined by the cutoff temperature, as specified in Fig. 6, while the energy capacity for an ideal water tank Q_{SWS} serves as the benchmark, which is the same as the theoretical energy of a water tank $Q_{0,w}$. A larger E_{st} means that a better stratification performance exists and thus the thermal storage tank is more efficient. In addition, the discharge power \dot{Q} is measured by the ratio of effective energy over the effective time as shown in Eq. (13), which indicates the heat transfer rate during the discharging process.

$$Q_{\text{SWS}} = Q_{0,w} = \rho_w c_{p,w} V (T_{\text{in}} - T_0) \quad (11)$$

$$E_{\text{st}} = \frac{Q_{\text{eff}}}{Q_{\text{SWS}}} \quad (12)$$

$$\dot{Q} = \frac{Q_{\text{eff}}}{t_{\text{eff}}} \quad (13)$$

3. Results and analysis

3.1. Discharging behavior

The results of the validated 3D numerical model, when the flow rate is 0.401 L/min, are exhibited and analyzed in this section to demonstrate the dynamic discharging behavior of the phase change emulsion stratification tank.

Fig. 7 presents the transient temperature distribution at the symmetry plane of the thermal storage tank, over the dimensionless time of 0.1–1.0. Hot emulsion enters from the sidewall close to the top surface,

and the cold emulsion exits from the bottom surface of the tank. In Fig. 7 (a), it can be observed that under the effect of buoyancy force, hot emulsion from the inlet is driven upwards to the top surface. Meanwhile, at the beginning of discharging, the inlet jet flow causes a certain degree of destratification when mixing with the cold emulsion in the tank. The mixing could be mainly due to the diffusion between hot and cold emulsion, as the flow rate is small here, according to the Reynolds number of 45 at the inlet. As time passes by, the developed thermocline separates the hot and cold emulsion, and then moving down to the bottom of the tank, as shown in Fig. 7 (b)-(d). When $t^* = 1.0$, the cold emulsion in the tank at the start has been fully replaced by the hot emulsion flowing into the storage tank. At this time, the temperature of most emulsion in the tank is close to the inlet temperature.

Fig. 8 captures the evolution of phase change in emulsion, which is characterized by the effective specific heat capacity $c_{p,\text{eff}}$. When the emulsion temperature is either lower or higher than the range of phase change temperature, $c_{p,\text{eff}}$ is taken from the fluid property 3700 J/(kg·K). This could happen when PCM in emulsion remains as the solid state close to the outlet, or when PCM in the emulsion is completely melted after absorbing heat in the chamber through ceiling panels and returned to the tank inlet, shown as the blue area in Fig. 8. The red area, separating solid and liquid PCM in emulsion, is where the emulsion is undergoing the phase change process. The latent heat is considered in $c_{p,\text{eff}}$ through being averaged over the temperature range, and $c_{p,\text{eff}}$ in phase change region is over four times of the emulsion specific heat capacity. During the discharging process, hot emulsion replaces the cold one in the tank, driving the red phase change region to move towards the tank bottom. It can be seen that even when cold emulsion has been fully displaced, i.e. $t^* = 1.0$, the outlet emulsion remains blue. This means that the emulsion flowing out of the storage tank can still utilize the latent heat in fluid while it cools down the temperature of ceiling temperature. But it should be noted that the outlet temperature is already above the cutoff temperature and discharge at this point is regarded as ineffective.

To characterize the temperature evolution of stratified layers inside the tank in experiments, temperature profiles of phase change emulsion and water storage tanks under different flow rates are plotted and compared in Fig. 9. The scatter points show the average values of three

repeated tests and the error bars indicate the corresponding standard deviations. The x-axis is the dimensionless time t^* normalized by the displacement time. The sensor T1 to T4 were arranged from high to low positions along the same vertical line, as shown in Fig. 2.

For both phase change emulsion and water, the figure shows that the temperature of each stratified layer increased steadily from the initial temperature towards inlet temperature, as the inflow of hot fluid replaced the cold fluid gradually. The temperature at the upper layers increased more rapidly due to closer to the inlet and thus the fluid was replaced earlier than the one closer to the outlet. It should be noted that from Fig. 9 (a) to (d), the rising rate of each stratified layer's temperature increased with the increasing flow rate. In other words, the temperature increased faster under a higher flow rate, for both emulsion and water. Specifically, at the end of discharging when $t^* = 1$, with the increase of flow rate, the temperature of T4 increased from around 12 °C to 14 °C. This is because a higher flow rate resulted in more fluid mixing and thus the destratification of the storage tank. The cold fluid at the bottom could not maintain a low temperature when experiencing a higher level of mixing under a large flow rate.

In general, no significant temperature difference between emulsion and water can be observed. Thus, it can be concluded that a PCE storage tank shares similar stratification characteristics with a conventional water storage tank. However, apart from the similarity, it could still be seen that at the lowest flow rate of 0.242 L/min, T3 and T4 of water was rising slightly more slowly than the ones of emulsion. In contrast, when the flow rate is higher, such as 0.370 L/min and 0.401 L/min, phase change emulsion began to exhibit a slower temperature increase, which is more significant for T4. This could be explained by the trade-off between buoyancy force and shear force. When the flow rate was high, the hot and cold fluid mixing induced was significant. In this case, the higher viscosity of phase change emulsion played an important role in reducing the mixing level owing to a higher shear force, which slowed down the temperature rising rate of cold fluid. On the other hand, buoyancy force became more dominant when the flow rate is low. The density change in a certain temperature range of emulsion is smaller than that of water, as in emulsion PCM remains in the solid state before melting and the base fluid is water. Hence, water experienced a larger

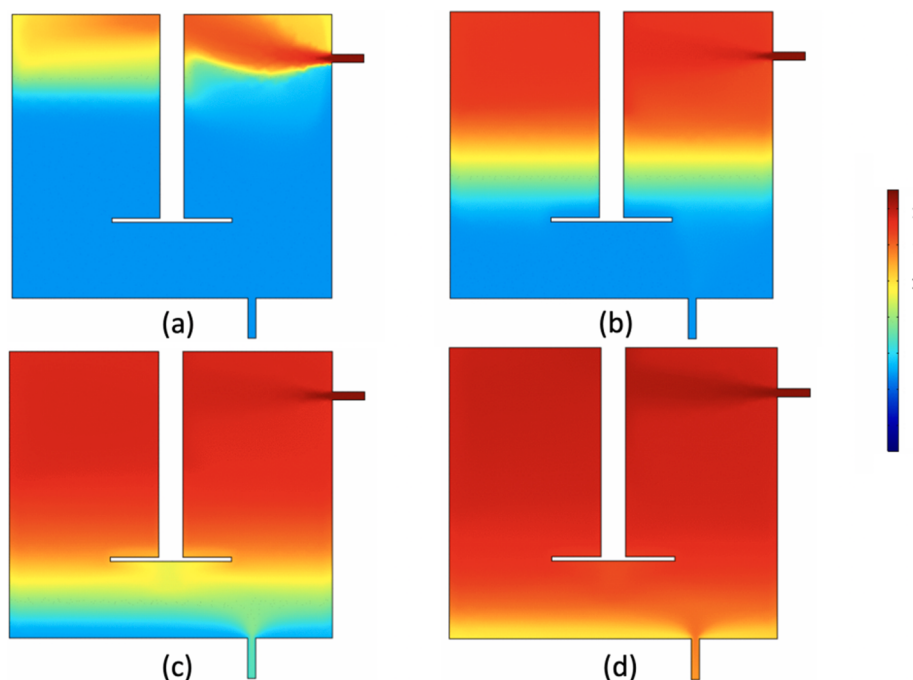


Fig. 7. Temperature contours inside the emulsion storage tank at the symmetry plane (unit: °C): (a) 587 s, $t^* = 0.1$; (b) 2645 s, $t^* = 0.4$; (c) 4702 s, $t^* = 0.7$; (d) 6612 s, $t^* = 1.0$.

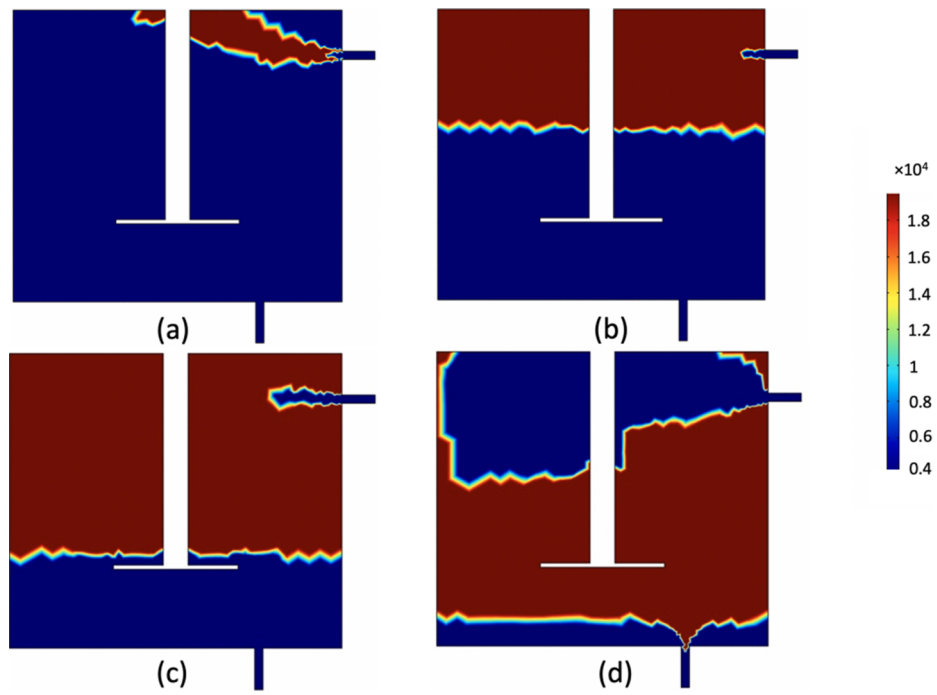


Fig. 8. The effective specific heat capacity inside the emulsion storage tank at the symmetry plane (unit: J/(kg·K)): (a) 587 s, $t^* = 0.1$; (b) 2645 s, $t^* = 0.4$; (c) 4702 s, $t^* = 0.7$; (d) 6612 s, $t^* = 1.0$.

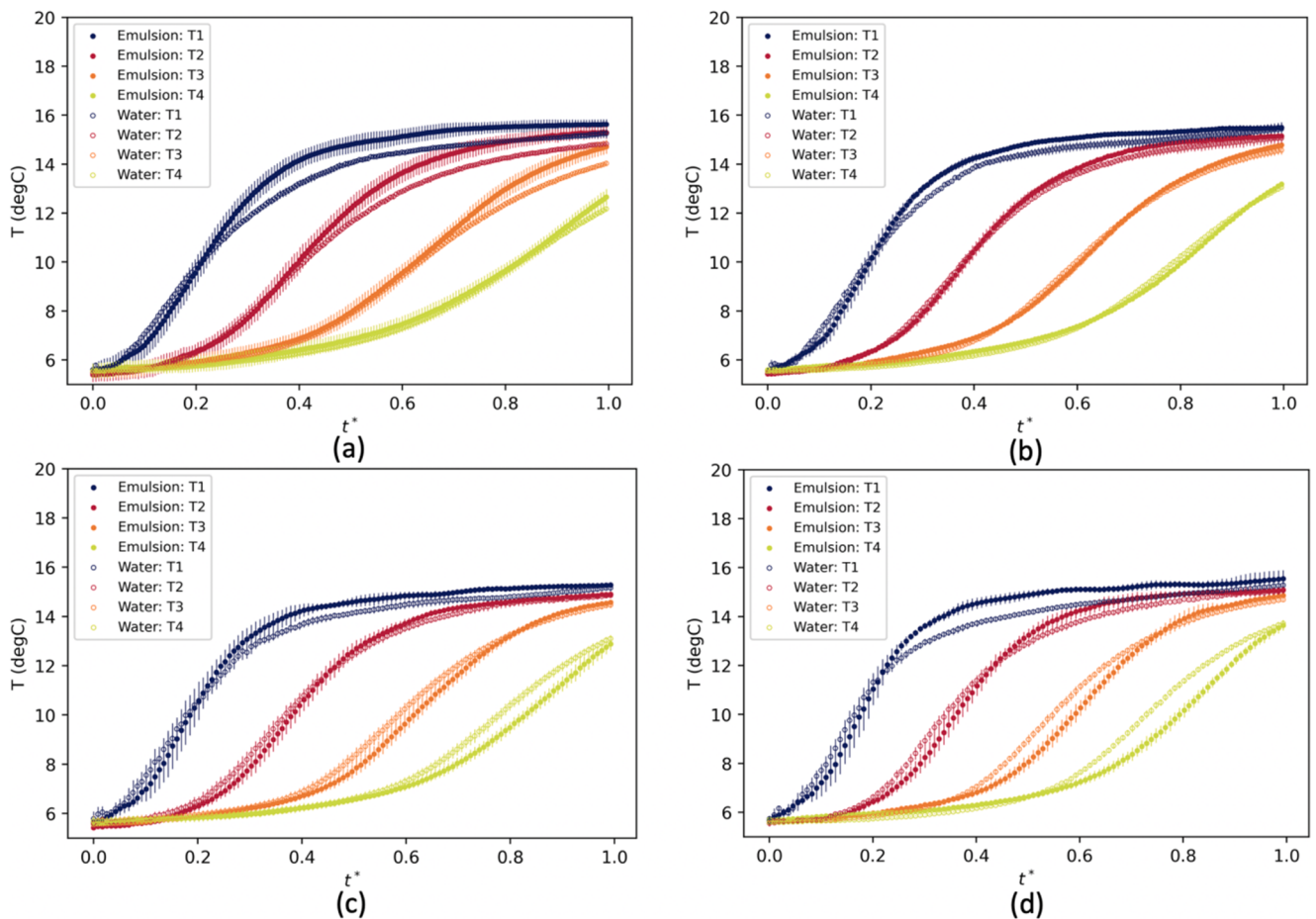


Fig. 9. Temperature profiles of phase change emulsion and water storage tanks under different flow rates in experiments: (a) 0.242 L/min; (b) 0.296 L/min; (c) 0.370 L/min; (d) 0.401 L/min.

buoyancy force, which is beneficial to thermal stratification, and the temperature closer to the outlet increased more slowly than the one of emulsion, as shown in Fig. 9 (c) and Fig. 9 (d).

3.2. Stratification performance

Based on the described cutoff temperature condition in Section 2, the dimensionless effective time t^*_{eff} and effective energy Q_{eff} can be determined under different fluid flow rates. In experiments, both phase change emulsion and water were tested as the storage medium for the stratification tank. Fig. 10 exhibits the effective energy efficiency Q_{eff}/Q_0 of emulsion and water, under different discharge rates, which has been normalized by the volume of the tank. It should be noted that the theoretical energy Q_0 is different for emulsion water. Though each set of experiments were repeated three times, only the data from the first group were selected to perform the energy analysis. This is because in the following repeated experiments, the phase change temperature range of emulsion could shift and be different from the measured value at the beginning.

It could be observed that when the normalized flow rate is increasing, the effective energy efficiency firstly increases and then decreases, for both phase change emulsion and water. The decreasing effective energy efficiency can be explained by the fact that increasing inlet velocity induces a higher level of mixing between the hot and cold fluid in the tank, which is undesirable for stratification. The decreasing trend is more obvious for water as the flow rate reaches higher values in experiments. For example, when the normalized flow rate rises by 58% from 1.4×10^{-4} to $2.2 \times 10^{-4} \text{ s}^{-1}$ for water, the dimensionless effective time reduces by 23%. However, at lower flow rates, even though mixing level increases with increasing \dot{V}/V , the effect of mixing on t^*_{eff} is taken over by the influence of tank heat loss to the environment. When the experimental storage tank was placed in the laboratory for 5 h, the water temperature increased from 5.4°C to 8.2°C . Considering that the air temperature in the room is 22.5°C , the thermal resistance of the tank can be calculated by the heat loss and the temperature difference between the room and storage tank, which is 0.54°C/W . In the discharging experiments, when the normalized flow rate for emulsion is as low as $0.7 \times 10^{-4} \text{ s}^{-1}$, the total displacement time is close to 4 h. In comparison, as \dot{V}/V increases to $1.4 \times 10^{-4} \text{ s}^{-1}$, the total displacement time drops by half to around 2 h. Consequently, the heat loss estimated by thermal resistance $Q_{\text{loss}} = R_{\text{tank}} \Delta T \cdot t$ would be higher for a lower flow rate, as the operation time is larger. This can explain the increasing trend of dimensionless effective time when \dot{V}/V increases until $1.4 \times 10^{-4} \text{ s}^{-1}$ for both emulsion and water.

The figure shows that the effective energy efficiency of phase change emulsion was slightly higher than the one of water, particularly when

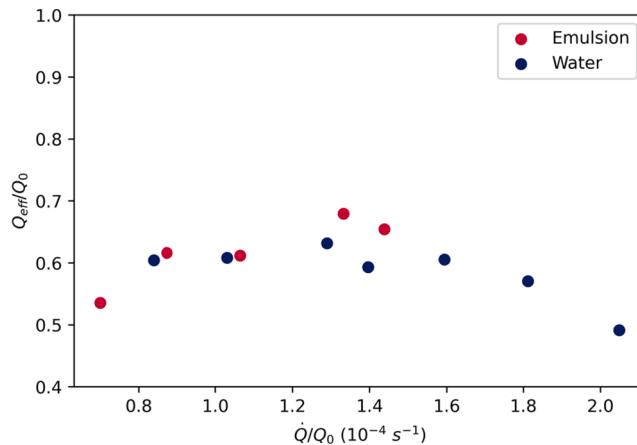


Fig. 10. The effective energy efficiency over normalized discharge rate.

the flow rate is larger. This could be contributed by the higher viscosity of emulsion, which inhibited the fluid mixing and slowed down the temperature increase rate at the outlet, as shown in Fig. 9 (c)-(d). Through stratification performance analysis and comparison with water in experiments, as a novel thermal energy storage medium, phase change emulsion shows its potential in thermal stratification inside a storage tank.

3.3. Enhancement with baffle plates

In this section, numerical simulation and analyses have been carried out to investigate the impact of different baffle plates design on enhancing the thermal stratification in the phase change emulsion storage tank. Following the effective specific heat capacity approach used in the validated numerical model for phase change emulsion, the simulation domain is simplified to a 2D axisymmetric plane with inlet and outlet at the centerline of the tank, shown in Fig. 11. The purpose is to speed up the simulation process and to generate a larger amount of data, to illustrate the concept of improving stratification with plates and to capture the characteristic thermal stratification enhancement at higher flow rates. Such high flow rate cannot be performed in our experiments, but will be relevant in other practical systems with higher cooling demands. Except that the inlet emulsion flow rate varies in parametric studies, the initial conditions, boundary conditions and other model settings are the same as the one in the validated 3D model, which is consistent with the values in experiments. The grid element number varies from 9634 to 30,626, depending on the set-up parameters. When the flow rate changes, the Reynolds number of inlet emulsion is always under 1000, meaning that the flow condition is laminar.

Systematic numerical simulations are performed for different plate sizes, plate positions and aspect ratios of the storage tank. As shown in Fig. 11, a horizontal circular baffle plate made of stainless steel with a diameter of d_p , is placed at a distance h_p away from the top of the tank. Hence, the inlet flow can impinge with the baffle and thus reduce the mixing due to jet flow, which would enhance thermal stratification. The plate size is indicated by a dimensionless diameter ratio of the plate over inlet tube d_p/d_i , while the plate position can be measured by the dimensionless ratio of the distance to the top of the tank over the inlet

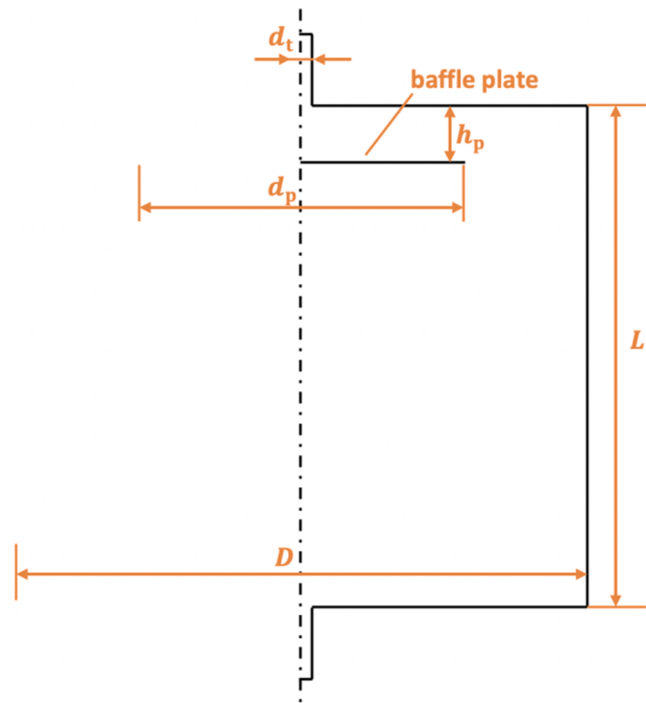


Fig. 11. The simulation domain and parameters concerned with baffle plates.

tube diameter h_p/d_t . As for the aspect ratio of the tank, it is calculated as tank height over tank diameter L/D .

To investigate the position of the baffle plate on the stratification and effective energy efficiency, the inlet tube diameter is fixed at 15 mm and h_p/d_t changes from 1 to 10 by varying the distance between the plate and top of the tank h_p . The flow rate, tank aspect ratio and diameter ratio of the plate over tube are fixed at 0.4 L/min, 0.87 L/min and 3 L/min, respectively. The results of the effective energy efficiency Q_{eff}/Q_0 are summarized in Table 2. It can be concluded that as the baffle plate moves closer to the inlet, the effective energy efficiency increases. This is because a smaller h_p/d_t can prevent the mixing from happening at an earlier stage during discharging, by making hot fluid from the inlet stay at the top of the tank. Importantly, when h_p/d_t drops from 2 to 1, no further enhancement in Q_{eff}/Q_0 can be observed. Therefore, h_p/d_t is set as 2 in the following investigation on the baffle plate size.

Fig. 12 exhibits the effects of the baffle plate size on the effective energy efficiency under different flow rates, when h_p/d_t and tank aspect ratio L/D are fixed. The inlet tube diameter d_t is kept as 15 mm and d_p/d_t changes by varying the baffle plate diameter d_p . Under a certain flow rate, Q_{eff}/Q_0 increases as d_p/d_t increases. Fig. 13 exhibits how different plate sizes influence the thermal stratification of emulsion when the flow rate is 1 L/min, which could help understand the variation of the effective energy efficiency. In Fig. 13 (a), when the tank is without a baffle plate, hot emulsion directly mixes with the cold one along the centerline after entering the tank and there exists no thermocline, which is undesirable for stratification. After applying a plate with a diameter same as the tube diameter, the thermocline starts to appear, even though there exists obvious mixing in the hot fluid region at the top of the tank, shown in Fig. 13 (b). As the plate size grows, the mixing is reduced and the stratification is improved. It could be seen that the thermocline in Fig. 13 (d) moves more slowly than the one in Fig. 13 (c).

As shown in Fig. 12 when there is no baffle plate ($d_p/d_t = 0$), the discrepancies of efficiency among different flow rates are significant. However, it could be seen that the differences are reduced with baffle plates introduced and when the diameter ratio of plate and tube d_p/d_t is large as 6, all three flow rates have nearly the same effective energy efficiency of around 0.75. Under this circumstance, the plate area over the cross-section area of the tank is 5%, which means that even a small plate would have an effective impact on enhancing the stratification of an emulsion tank to a desirable level. Apart from adding baffle plates in the tank, increasing the tank aspect ratio could improve thermal stratification. For instance, when the flow rate is 0.4 L/min, changing L/D from the original 0.87 to 1.5 can increase the effective energy efficiency by 13%, from 0.71 to 0.8.

The plotted data in Fig. 12 are fitted into an exponential correlation, shown as

$$\frac{Q_{\text{eff}}}{Q_0} = -ae^{-1.1\left(\frac{d_p}{d_t}\right)} + 0.75. \quad (14)$$

The empirical correlation predicts the effective energy efficiency of phase change emulsion storage tank, when the diameter of the baffle plate d_p is varying. The R-squares of three fitted curves are all over 0.99, which shows the validity of fitting. The coefficient a is determined by the flow rate and indicates the increasing rate of efficiency with increasing

Table 2
The effective energy efficiency under different positions of the baffle plate.

h_p/d_t	Q_{eff}/Q_0
1	0.75
2	0.75
3	0.74
5	0.72
10	0.70

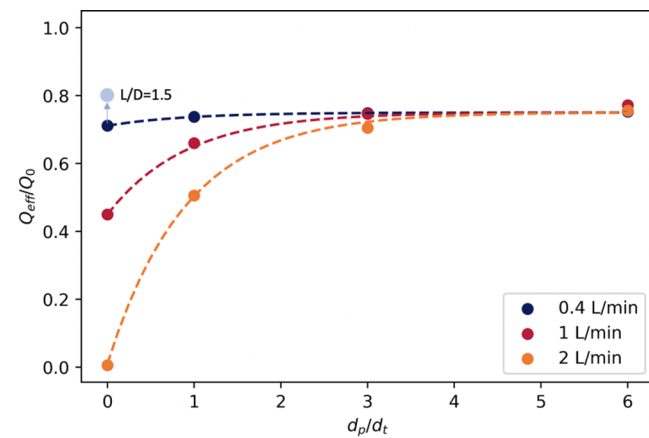


Fig. 12. The effective energy efficiency vs d_p/d_t under different flow rates ($h_p/d_t = 2, L/D = 0.87$).

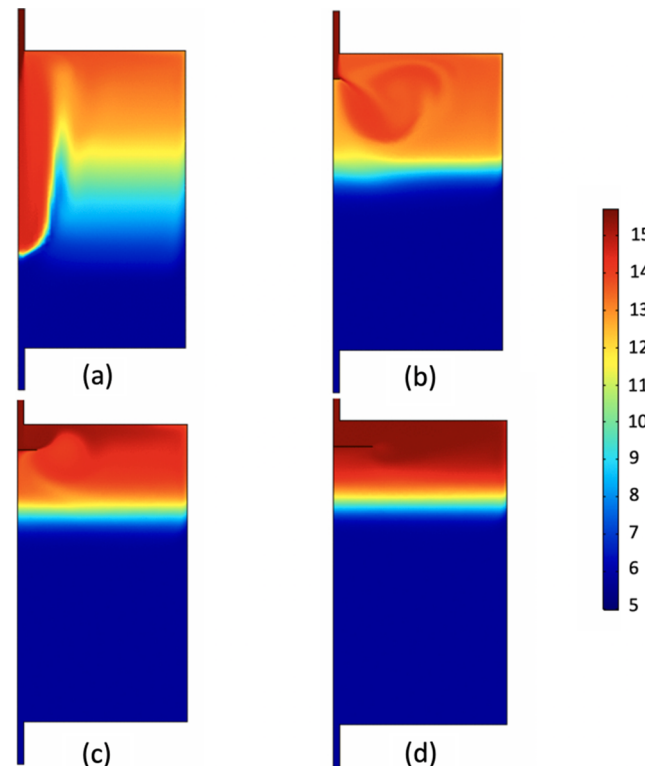


Fig. 13. Temperature contours of phase change emulsion under different baffle plate sizes when $t^* = 0.5$, flow rate = 1 L/min (unit: °C): (a) $d_p/d_t = 0$, no baffle plate; (b) $d_p/d_t = 1$; (c) $d_p/d_t = 3$; (d) $d_p/d_t = 6$.

baffle plate diameter, which is summarized in Table 3. When there is no baffle plate placed in the tank, d_p/d_t equals to zero, and thus the initial effective energy efficiency $(Q_{\text{eff}} - Q_0)_{\text{initial}}$ is $0.75 - a$. When d_p/d_t rises to infinite, the ultimate effective energy efficiency $(Q_{\text{eff}} - Q_0)_{\infty}$ is the constant term 0.75. The constant can be viewed as the maximum efficiency, which could be affected by the cutoff temperature and tank aspect ratio. For example, if the cutoff temperature is assumed to be higher, it could be expected that the constant would increase, since more energy would be available to cool down the ceiling panels. On the other hand, as shown in Fig. 12, if the tank aspect ratio increases, the efficiency would increase correspondingly, and it could be expected that the upper limit would increase. The correlation could serve as guidance on choosing proper size of baffle plate to achieve a desirable effective

Table 3The coefficient a under different flow rates.

Flow rate (L/min)	Coefficient a
0.4	0.039
1	0.30
2	0.74

energy efficiency of a phase change emulsion storage tank.

3.4. Effective energy ratio

The experimental and numerical results of effective energy ratio E_{st} for phase change emulsion and water are summarized in Fig. 14, by using the theoretical energy of an ideal stratified water storage tank Q_{SWS} as the benchmark. As a result, the blue dashed line, representing E_{st} of the SWS tank, has a value of 1. Similarly, the red dashed line indicates the effective energy ratio of a perfectly stratified phase change emulsion tank, i.e. the theoretical energy ratio of emulsion tank over the one of the water tank $Q_{0,e}/Q_{0,w}$. The corresponding value means that the theoretical energy capacity of phase change emulsion is 1.6 times that of water. It should be noticed that if the supercooling of the emulsion can be reduced, the operating temperature range can be shortened. Under the circumstance, the contribution of latent heat to energy storage would be more significant and thus theoretical E_{st} of emulsion tank can be more than 2 times that of water.

In the figure, the x-axis is the discharging rate normalized by the theoretical energy Q_0 . The scatter points exhibit the effective energy ratio of tests in experiments. It can be seen that as the stratification in the tank was not perfect, E_{st} of both emulsion and water did not reach the theoretical value. Under the circumstance, the phase change emulsion tanks showed higher E_{st} than that of water tanks. As the effective energy efficiencies of emulsion tanks were slightly higher than water tanks under the same flow rate, as shown in Fig. 10, it could be concluded that the effective energy ratio E_{st} of phase change emulsion was more than 1.6 times that of water under practical operation. When the flow rate for emulsion was largest in the experiment, E_{st} of emulsion could reach 1.7 times that of water. The red shaded regions highlight the numerical results of phase change emulsion stratification enhancement by using baffle plates, as explained in Section 3.3. Numerical simulation captures the stratification and thermal storage behavior under high flow rates, which cannot be achieved in our experiments. It shows the potential of increasing E_{st} of a stratified emulsion storage tank through thermal stratification enhancement.

From the experiment results, it can be concluded that the effective energy ratio E_{st} of a stratified storage tank with phase change emulsion does not have significant fluctuations under varying flow rates. Even

enough when more mixing would occur at higher flow rates, baffle plates have been approved to be effective in reducing the mixing level, improving thermal stratification and thus increasing E_{st} . This could be an advantage of phase change emulsion, as the effective energy ratio E_{st} of a traditional shell-and-tube PCM thermal energy storage can be easily affected by the flow rate, especially when the effective thermal conductivity of PCM is low [39]. Hence, the energy performance of a stratified phase change emulsion tank is less likely to be influenced by the flow rate, which shows the flexibility in operation. Besides, installing baffle plates to enhance performance seems to be an easier way in comparison to enhancing the thermal conductivity with fins or highly conductive materials in the shell-and-tube design.

4. Conclusions

Previously published studies on PCM emulsions have been mainly focused on their uses as heat transfer fluid and the related heat transfer and flow characteristics. The present study tested the thermal stratification and energy performance with the PCM emulsion as both the storage medium and heat transfer fluid. An experimental system was built up to study the novel PCM emulsion stratification tank for a radiant cooling scenario. Numerical simulation was performed to understand the thermal stratification inside the tank and to guide the performance improvement with baffle plates. According to the experimental and numerical results, the following conclusions can be drawn.

- The effective energy ratio E_{st} of PCE tank was 1.6–1.7 times that of an SWS tank, suggesting that the PCM emulsion can effectively reduce the volume of a thermally stratified storage tank, contributed by the latent heat absorbed during the discharging process.
- The PCM emulsion and water showed similar discharging behavior and stratification performance in experiments, in terms of dimensionless effective time t^*_{eff} and effective energy efficiency Q_{eff}/Q_0 .
- The baffle plates can effectively increase the effective energy efficiency of the stratified PCM emulsion storage tank up to 1.3, especially at higher flow rates, surpassing the one of an ideally stratified SWS tank. A small plate with an area of around 5% of the tank cross-section area can noticeably improve thermal stratification and enhance the effective energy efficiency to around 0.75.
- Traditional latent heat TES systems like shell-and-tube units normally requires heat transfer enhancement on the PCM side to reduce the thermal resistance. Otherwise, the effective energy capacity would be greatly affected by the charging and discharging rate. In comparison, the proposed stratified phase change emulsion tank is more flexible as the fluctuation of the flow rate had no significant impact on the effective energy when the baffle plate is placed to reduce fluid mixing.

The study presented a stratified PCM emulsion tank that enables effective energy performance for a cold storage application with radiant cooling panels. Both experimental and numerical results contribute to a better understanding of the heat transfer and energy performance of PCM emulsion. This work shows the potential of PCM emulsion being employed in energy storage, cooling/heating and other applications, and paves the way for future application and design of a stratified PCM emulsion storage tank.

CRediT authorship contribution statement

Haobin Liang: Conceptualization, Methodology, Validation, Investigation, Resources, Data curation, Writing – original draft, Visualization. **Liu Liu:** Conceptualization, Methodology, Validation, Investigation, Resources, Data curation, Writing – review & editing. **Ziwen Zhong:** Methodology, Resources, Writing – review & editing. **Xixiang Gan:** Conceptualization, Methodology, Resources, Writing – review & editing, Supervision. **Jian-Yong Wu:** Conceptualization,

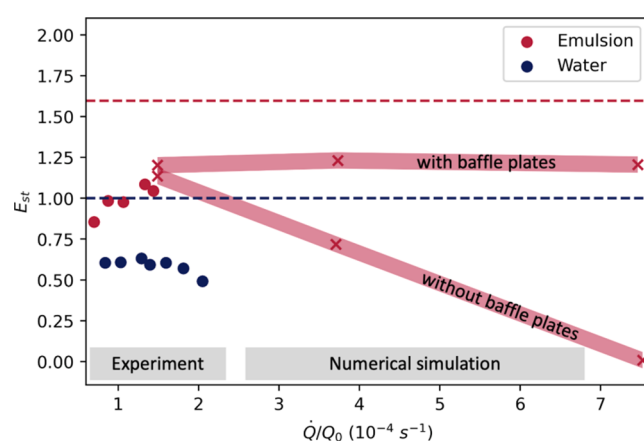


Fig. 14. The effective energy ratio E_{st} of phase change emulsion and water.

Methodology, Resources, Writing – review & editing, Supervision, Funding acquisition. Jianlei Niu: Conceptualization, Methodology, Resources, Writing – review & editing, Supervision, Funding acquisition.

Declaration of Competing Interest

The authors declare that they have no known competing financial interests or personal relationships that could have appeared to influence the work reported in this paper.

Acknowledgements

This work was supported financially by the Environment and Conservation Fund (ECF Project 53/2018), and by the Hong Kong Polytechnic University. The authors are grateful to Jing Li's support to the design and construction of the test rig.

References

- [1] Nazir H, Batool M, Bolivar Osorio FJ, Isaza-Ruiz M, Xu X, Vignarooban K, et al. Recent developments in phase change materials for energy storage applications: A review. *Int J Heat Mass Transf* 2019;129:491–523.
- [2] Wang X, Niu J, van Paassen AHC. Raising evaporative cooling potentials using combined cooled ceiling and MPCM slurry storage. *Energy Build* 2008;40(9): 1691–8.
- [3] Zhang S, Niu J. Cooling performance of nocturnal radiative cooling combined with microencapsulated phase change material (MPCM) slurry storage. *Energy Build* 2012;54:122–30.
- [4] Liu L, et al. State-of-the-art on thermal energy storage technologies in data center. *Energy Build* 2020;226:110345.
- [5] Han YM, Wang RZ, Dai YJ. Thermal stratification within the water tank. *Renew Sustain Energy Rev* 2009;13(5):1014–26.
- [6] Fertahi S-Din, Jamil A, Benbassou A. Review on Solar Thermal Stratified Storage Tanks (STSST): Insight on stratification studies and efficiency indicators. *Sol Energy* 2018;176:126–45.
- [7] Wang S, Davidson JH. Selection of permeability for optimum performance of a porous tube thermal stratification manifold. *Sol Energy* 2015;122:472–85.
- [8] Lou W, Fan Y, Luo L. Single-tank thermal energy storage systems for concentrated solar power: Flow distribution optimization for thermocline evolution management. *J Storage Mater* 2020;32:101749.
- [9] Altuntop N, Arslan M, Ozceyhan V, Kanoglu M. Effect of obstacles on thermal stratification in hot water storage tanks. *Appl Therm Eng* 2005;25(14–15):2285–98.
- [10] Bouhal T, Fertahi S, Agrouaz Y, El Rhafiki T, Kousksou T, Jamil A. Numerical modeling and optimization of thermal stratification in solar hot water storage tanks for domestic applications: CFD study. *Sol Energy* 2017;157:441–55.
- [11] Erdemir D, Altuntop N. Improved thermal stratification with obstacles placed inside the vertical mantled hot water tanks. *Appl Therm Eng* 2016;100:20–9.
- [12] Zachár A, Farkas I, Szlivkó F. Numerical analyses of the impact of plates for thermal stratification inside a storage tank with upper and lower inlet flows. *Sol Energy* 2003;74(4):287–302.
- [13] Wang Z, Zhang H, Dou B, Huang H, Wu W, Wang Z. Experimental and numerical research of thermal stratification with a novel inlet in a dynamic hot water storage tank. *Renewable Energy* 2017;111:353–71.
- [14] García-Mari E, Gasque M, Gutiérrez-Colomer RP, Ibáñez F, González-Altozano P. A new inlet device that enhances thermal stratification during charging in a hot water storage tank. *Appl Therm Eng* 2013;61(2):663–9.
- [15] Deng Y, et al. Performance assessment of a novel diffuser for stratified thermal energy storage tanks – The nonequal-diameter radial diffuser. *J Storage Mater* 2021;35:102276.
- [16] Li S-H, Zhang Y-X, Li Y, Zhang X-S. Experimental study of inlet structure on the discharging performance of a solar water storage tank. *Energy Build* 2014;70: 490–6.
- [17] Chandra YP, Matuska T. Numerical prediction of the stratification performance in domestic hot water storage tanks. *Renewable Energy* 2020;154:1165–79.
- [18] Iversen S, Lin W. Numerical simulation of three-dimensional flow dynamics in a hot water storage tank. *Appl Energy* 2009;86(12):2604–14.
- [19] Woods J, Mahvi A, Goyal A, Kozubal E, Odukomiaya A, Jackson R. Rate capability and Ragone plots for phase change thermal energy storage. *Nat Energy* 2021;6(3): 295–302.
- [20] Liang H, Niu J, Gan Y. Performance optimization for shell-and-tube PCM thermal energy storage. *J Energy Storage* 2020;30:101421.
- [21] Cherathathan M, Velraj R, Renganarayanan S. Heat transfer and parametric studies of an encapsulated phase change material based cool thermal energy storage system. *J Zhejiang Univ - Sci A* 2006;7(11):1886–95.
- [22] Wang F, Lin W, Ling Z, Fang X. A comprehensive review on phase change material emulsions: Fabrication, characteristics, and heat transfer performance. *Sol Energy Mater Sol Cells* 2019;191:218–34.
- [23] Zhang X, Wu J-Y, Niu J. PCM-in-water emulsion for solar thermal applications: The effects of emulsifiers and emulsification conditions on thermal performance, stability and rheology characteristics. *Sol Energy Mater Sol Cells* 2016;147 (Supplement C):211–24.
- [24] Chen J, Zhang P. Preparation and characterization of nano-sized phase change emulsions as thermal energy storage and transport media. *Appl Energy* 2017;190: 868–79.
- [25] Liu L, Niu J, Wu J-Y. Formulation of highly stable PCM nano-emulsions with reduced supercooling for thermal energy storage using surfactant mixtures. *Sol Energy Mater Sol Cells* 2021;223:110983.
- [26] Wang F, Zhang C, Liu J, Fang X, Zhang Z. Highly stable graphite nanoparticle-dispersed phase change emulsions with little supercooling and high thermal conductivity for cold energy storage. *Appl Energy* 2017;188:97–106.
- [27] Morimoto T, Togashi K, Kumano H, Hong H. Thermophysical properties of phase change emulsions prepared by D-phase emulsification. *Energy Convers Manage* 2016;122:215–22.
- [28] Huang L, Petermann M. An experimental study on rheological behaviors of paraffin/water phase change emulsion. *Int J Heat Mass Transf* 2015;83:479–86.
- [29] Zhang X, Niu J, Wu J-Y. Development and characterization of novel and stable silicon nanoparticles-embedded PCM-in-water emulsions for thermal energy storage. *Appl Energy* 2019;238:1407–16.
- [30] Ma F, Chen J, Zhang P. Experimental study of the hydraulic and thermal performances of nano-sized phase change emulsion in horizontal mini-tubes. *Energy* 2018;149:944–53.
- [31] Morimoto T, Kumano H. Flow and heat transfer characteristics of phase change emulsions in a circular tube: Part 1. Laminar flow. *Int J Heat Mass Transf* 2018;117 (Supplement C):887–95.
- [32] Ho CJ, et al. Thermal performance of phase change nano-emulsion in a rectangular minichannel with wall conduction effect. *Int Commun Heat Mass Transfer* 2020; 110:104438.
- [33] Delgado M, Lázaro A, Mazo J, Peñalosa C, Dolado P, Zalba B. Experimental analysis of a low cost phase change material emulsion for its use as thermal storage system. *Energy Convers Manage* 2015;106:201–12.
- [34] Shao J, Darkwa Jo, Kokogiannakis G. Review of phase change emulsions (PCMEs) and their applications in HVAC systems. *Energy Build* 2015;94:200–17.
- [35] Feng J, et al. Performance enhancement of a photovoltaic module using phase change material nanoemulsion as a novel cooling fluid. *Sol Energy Mater Sol Cells* 2021;225:111060.
- [36] Wang F, et al. Experimental and simulative investigations on a phase change material nano-emulsion-based liquid cooling thermal management system for a lithium-ion battery pack. *Energy* 2020;207:118215.
- [37] Oró E, de Gracia A, Castell A, Farid MM, Cabeza LF. Review on phase change materials (PCMs) for cold thermal energy storage applications. *Appl Energy* 2012; 99:513–33.
- [38] Agyenim F, Hewitt N, Eames P, Smyth M. A review of materials, heat transfer and phase change problem formulation for latent heat thermal energy storage systems (LHTESS). *Renew Sustain Energy Rev* 2010;14(2):615–28.
- [39] Fang Y, et al. Experimental study of storage capacity and discharging rate of latent heat thermal energy storage units. *Appl Energy* 2020;275:115325.
- [40] Gaedtke M, et al. Total enthalpy-based lattice Boltzmann simulations of melting in paraffin/metal foam composite phase change materials. *Int J Heat Mass Transf* 2020;155:119870.
- [41] Zauer C, Hengstberger F, Etzel M, Lager D, Hofmann R, Walter H. Experimental characterization and simulation of a fin-tube latent heat storage using high density polyethylene as PCM. *Appl Energy* 2016;179:237–46.
- [42] Fan L-W, Fang X, Wang X, Zeng Yi, Xiao Y-Q, Yu Z-T, et al. Effects of various carbon nanofillers on the thermal conductivity and energy storage properties of paraffin-based nanocomposite phase change materials. *Appl Energy* 2013;110:163–72.
- [43] Martinelli M, Bentivoglio F, Caron-Soupart A, Couturier R, Fournigue J-F, Marty P. Experimental study of a phase change thermal energy storage with copper foam. *Appl Therm Eng* 2016;101:247–61.
- [44] Yang X, Wei P, Cui X, Jin L, He Y-L. Thermal response of annuli filled with metal foam for thermal energy storage: An experimental study. *Appl Energy* 2019;250: 1457–67.
- [45] Fang Y, Niu J, Deng S. An analytical technique for the optimal designs of tube-in-tank thermal energy storage systems using PCM. *Int J Heat Mass Transf* 2019;128: 849–59.
- [46] COMSOL Multiphysics 5.5 Documentation.
- [47] Incropera FP, et al. *Fundamentals of heat and mass transfer*. Wiley; 2007.
- [48] Fang Y, Niu J, Deng S. Numerical analysis for maximizing effective energy storage capacity of thermal energy storage systems by enhancing heat transfer in PCM. *Energy Build* 2018;160:10–8.